Circuit Model for Substrate Resonance Coupling in Grounded Coplanar Waveguide Circuits

Robert W. Jackson

Abstract—**At high frequencies, grounded coplanar waveguide MMIC circuits can be prone to destructive intercircuit coupling effects due to substrate resonances. Analytic formulas for a simple circuit model of this coupling are presented in this paper. The model can be used with commercially available CAD in order to estimate the importance of such coupling for a particular circuit and substrate configuration. Results predicted by this model are compared to numerically rigorous spectral domain results and to experiment.**

I. Introduction

Grounded coplanar waveguide (GCPW) has recently been used in several MMIC circuits including one distributed amplifier operating up to 100 GHz [1]. GCPW's principle advantage is the location of the signal grounds on the same substrate surface as the signal line. This eliminates the need for via holes and thus simplifies the fabrication process. It also reduces the parasitic inductance that occurs in grounding active devices. GCPW circuits differ from conventional coplanar waveguide circuits in that GCPW has an additional conducting plane on the opposite side of the substrate from the circuit side. The most important purpose of this additional plane is to provide heat sinking, but it also provides shielding and support.

Unfortunately, parallel plate waves exist between the circuit plane and the lower ground plane. These waves can provide a means for undesirable coupling between GCPW circuit elements [2]–[5], [8]. Usually only the lowest order parallel plate wave, the TM_0 wave, is not cut off. It is TEM when the dielectric between the planes is uniform and non-TEM when the dielectric is nonuniform, as it is when two substrate layers with differing permittivity are present. The TM_0 parallel plate wave takes the place of the TM_0 surface wave which is always present in conventional coplanar waveguide [6]. GCPW energy couples into this wave at all circuits discontinuities and, for a strictly defined GCPW, also leaks from uniform transmission lines [2].

When the GCPW substrate is bounded laterally, TM_0 waves reflect off the boundaries and can add constructively or destructively at points within the substrate. If the reflection is strong and there is little loss in the substrate, circuits located in certain spots can experience enhanced coupling at resonance frequencies. If the lateral boundaries are conducting (as a result of ribbon bonds or conductive epoxy), it is clear that a dielectric filled rectangular cavity is formed between the side walls and top and bottom ground planes. This is illustrated in Fig. 1 where the cavity dimensions are $a \times b \times (d_1 + d_2)$. The cavity may resonate at a number of frequencies in a bandwidth depending on the electrical size of the substrate. The importance of the resonance with respect to circuit operation depends on the Q of the resonance and on the degree of coupling between various circuit elements and the resonant field.

A simple circuit model for substrate resonance coupling is presented in this paper. The circuit elements in the model are easily determined using analytic formulas which are derived starting from full wave analysis. No fitting parameters or lengthy numerical calculations are necessary. The resulting circuit model can be used with commercially available circuit CAD in order to estimate the importance of GCPW resonance effects for a particular circuit and substrate configuration. A similar type of model has been derived for coupling microstrip circuits to their packages [7].

Manuscript received October 1, 1992; revised February 8, 1993.

The author is with the Department of Electrical and Computer Engineering, University of Massachusetts, Amherst, MA 01003.

IEEE Log Number 9211866.

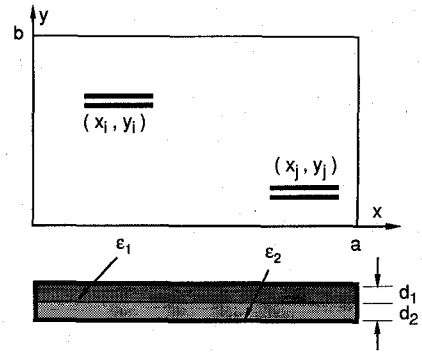

Fig. 1. Grounded coplanar waveguide on a substrate bounded by conducting sidewalls.

In the next section the theoretical derivation of the circuit model is described. In Section III a comparison to a full wave moment method solution is presented. In Section IV the model results are compared to experiment. Lastly, in Section V, the applicability and implications of the model are discussed.

II. Derivation of the Model

A. Mutual Admittance Near Resonance

Fig. 1 shows apertures in which electric fields E_{yi} and E_{yj} are supposed. The illustrated apertures are lengths of coplanar waveguide, but the derivation is only slightly modified for a length of slotline. The apertures are supported by two substrates with thickness d_1 and d_2 and dielectric constants ε_1 and ε_2. As stated previously, a cavity is formed by vertical perfectly conducting walls at $x = [0, a]$ and $y = [0, b]$ and the horizontal conductors at $z = [0, -(d_1 + d_2)]$. Above $z = 0$ the fields are unbounded. The mutual admittance between the ith and jth apertures is defined to be

$$Y_{ij} = -\frac{1}{V_i V_j} \iint dx\, dy\, E_{yi} J_{yj} \tag{1}$$

where

$$J_{yj} \equiv \Delta H_{xj} = H_{xj}^{+} - H_{xj}^{-}. \tag{2}$$

The fields H_{xj}^{+} and H_{xj}^{-} are the magnetic fields evaluated just above and below the $z = 0$ plane. They result from the E_y field in the jth aperture. V_i and V_j are voltages appropriate to the E field structure in the ith and jth apertures.

The model we are developing is valid near a resonance. And since this resonance occurs in the cavity located below $z = 0$, H_{xj}^{-} will be much larger than H_{xj}^{+}. We can relate the field H_{xj}^{-} to E_{yj} via a Green's function,

$$H_{xj}^{-}(x, y) = \iint dx'\, dy'\, G_{xx}(x, x', y, y')\, M_{xj}(x', y') \tag{3}$$

where $M_{x_j} \equiv -E_{yj}$ and G_{xx} is as defined in the Appendix. Inserting (3) into (2) and combining with (1) results in

$$Y_{ij} = \frac{1}{V_i V_j} \iint dx\, dy \left[-E_{yi} H_{xj}^{+} - E_{yi} \iint dx'\, dy'\, G_{xx} E_{yj} \right]. \tag{4}$$

Define the $f_i(x)$ and $g_i(y)$ to be the x and y dependence of E_{yi} such that $E_{yi} = f_i(x) g_i(y)$. Substitute these expressions and the

expression for G_{xx} into (4) to get

$$Y_{ij} = \frac{1}{V_i V_j} \sum_{n=1}^{\infty} \sum_{m=1}^{\infty} \frac{4}{abk_\rho^2} \left\{ \frac{k_x^2}{Z_E} + \frac{k_y^2}{Z_M} \right\} \cdot F_i(k_x) G_i(k_y) F_j(k_x) G_j(k_y) \tag{5a}$$

where

$$F_i(k_x) = \int dx\, f_i(x)\, \sin(k_x x) \tag{5b}$$

$$G_i(k_y) = \int dy\, g_i(y)\, \cos(k_y y) \tag{5c}$$

$$k_x = \frac{n\pi}{a}, \qquad k_y = \frac{m\pi}{b} \tag{6}$$

and we have neglected the H_{xj}^+ part of (4).

We now divide the summation in (5a) into resonant and nonresonant parts. For a specific choice of $\{n, m\}$ values, say $\{n', m'\}$, Z_E and Z_M can, in general, be zero at a number of frequencies corresponding to the $TE_{n'm'\ell}$ and $TM_{n'm'\ell}$ cavity modes (where $l = 0, 1, 2\cdots$). The substrates of interest to MIC and MMIC designers are thin enough that only the $TM_{n'm'0}$ mode will resonate. At frequencies near that resonance Z_M is small and the n', m' term in (5a) dominates. Thus the part of (5a) that dominates near a resonance is

$$Y_{ij}^R \equiv \frac{4k_y^2}{abk_\rho^2 Z_M} F_i(k_x) \frac{G_i(k_y)}{V_i} F_j(k_x) \frac{G_j(k_y)}{V_j} \Big|_{\substack{n=n' \\ m=m'}} . \tag{7}$$

Now define the real frequency ω_0 by

$$\mathrm{Im}[Z_M(\omega_0)] = 0 \tag{8}$$

and expand Z_M around ω_0 such that

$$Z_M(\omega) \approx \mathrm{Re}(Z_M)\Big|_{\omega=\omega_0} + j\, \mathrm{Im}[\partial Z_M/\partial\omega]\Big|_{\omega=\omega_0} (\omega - \omega_0) \tag{9}$$

where $\mathrm{Re}[\partial Z_M/\partial\omega](\omega - \omega_0)$ is assumed to be negligible. In cases where the substrate is low loss, $\mathrm{Re}(Z_M)$ is very small and near ω_0 (7) becomes very large. From this expressions one can determine a useful approximation for the cavity resonance Q,

$$Q \approx \frac{\omega_0}{2} \frac{\mathrm{Im}(\partial Z_M/\partial\omega)}{\mathrm{Re}(Z_M)} . \tag{10}$$

We can further simplify (7) by evaluating F_i and G_i in (5b) and (5c). Assume that the ith aperture is a short section of transmission line centered at $x = x_i$ with a length $\Delta\ell_i$. Then from (5b)

$$F_i(k_x) \approx f_i(x_i)\Delta\ell_i\, \sin k_x x_i . \tag{11}$$

In the case where the transmission line is a slot of width W centered at y_i

$$\frac{G_i(k_y)}{V_i} \approx \cos[k_y y_i] W/V_i \tag{12}$$

where $g_i(y)$ is assumed to be 1 within the slot. In the case where a section of CPW transmission line is centered at y_i with two slots of width W separated by a strip width S, $g(y)$ is assumed to be $+1$ within the slot located at $y > y_i$ and -1 within the slot located at $y < y_i$. After some manipulations we can approximate

$$\frac{G_i(k_y)}{V_i} \approx -k_y\, \sin[k_y y_i] W(S + W)/V_i . \tag{13}$$

We define the voltage $V_i \equiv f_i(x_i)W$ for both the slot and CPW.

Now insert expressions (9), (11), (12) or (13) into (7) to get

$$Y_{ij}^R \approx \frac{N_i N_j}{\mathrm{Re}(Z_M) + j\, \mathrm{Im}(\partial Z_M/\partial\omega)[\omega - \omega_0]} \tag{14a}$$

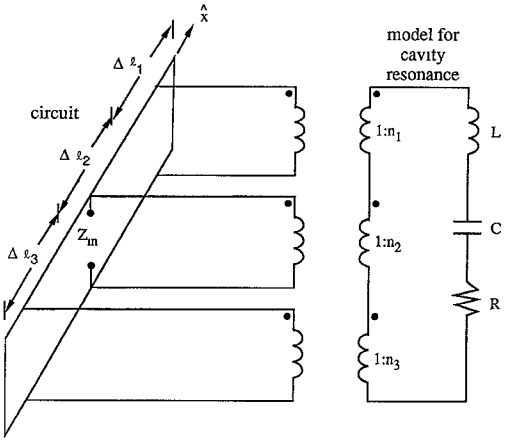

Fig. 2. A simple circuit consisting of a length of transmission line short circuited at the ends and driven in the middle. The RLC circuit and transformers model the substrate resonance effect.

where

$$N_\alpha = \frac{2}{\sqrt{ab}} \frac{k_y}{k_\rho} \Delta\ell_\alpha\, \sin(k_x x_\alpha)\, \cos(k_y y_\alpha) , \tag{14b}$$

for a single slot or

$$N_\alpha = \frac{-2}{\sqrt{ab}} \frac{k_y^2}{k_\rho} \Delta\ell_\alpha (S + W)\, \sin(k_x x_\alpha)\, \sin(k_y y_\alpha) , \tag{14c}$$

for a CPW.

B. Equivalent Circuit

Suppose a GCPW or slotline circuit to be made up of a number of sections of transmission line. In a conventional circuit theory analysis, $ABCD$ matrices, or other two-port matrices, can be used to couple these sections together to form a larger circuit. Package or substrate resonances add additional coupling which conventional circuit theory does not include.

All of these coupling effects are included in the rigorous method of moments (MoM) solution. In coplanar circuits MoM makes use of the mutual admittance Y_{ij} defined in (6). The effect of Y_{ij} excluding Y_{ij}^R is usually approximated by the conventional network theory solution. To include Y_{ij}^R in the network formulation we must include circuitry that approximates that effect.

Consider the topology illustrates in Fig. 2. The basic circuit in this example is a length of transmission line short circuited at both ends and excited at the center. The transmission line is divided into three sections where each section is connected at its end points to its neighbor with the typical network theory voltages and currents. The topology in the figure shows additional coupling via circuitry which models the resonant coupling term in (6). This includes the transformers and the series RLC circuit. Away from resonance the RLC circuit has a low admittance and, since the turns ratio of the transformers is normally very small (light coupling), the admittance seen looking to the right into the primary of each transformer is very small. At resonance, with a high Q cavity, the RLC admittance is very high allowing a large current to flow in the resonator circuit. This permits strong resonance coupling between circuit sections and supplements the conventional junction coupling. This topology was chosen with the aforementioned qualities in mind.

The admittance matrix for coupling from the ith primary to the jth primary of the resonance circuit model is

$$Y_{ij}^{RC} = \frac{n_i n_j}{R + j\left[\omega L - \frac{1}{\omega C}\right]} \approx \frac{n_i n_j}{R + j2L\left[\omega - \frac{1}{\sqrt{LC}}\right]} \tag{15}$$

where the approximation is the usual one for frequencies near resonance.

The analytic expressions for R, L, C, n_i can now be determined by comparing Y^{RC} in (15) with Y^R in (14). Thus,

$$L = \frac{1}{2}\,\mathrm{Im}\left(\frac{\partial Z_M}{\partial \omega}\right)\Big|_{\omega_0} \longrightarrow (\mu_0 d) \tag{16a}$$

$$C = \frac{1}{L\omega_0^2} \tag{16b}$$

$$R = \mathrm{Re}(Z_M)\Big|_{\omega_0} = \omega_0 L/Q \longrightarrow \left(\omega_0 L\varepsilon''/\varepsilon'\right) \tag{16c}$$

$$n_\alpha = N_\alpha \tag{16d}$$

where Q is the unloaded Q of the substrate cavity and the arrows show the simplification for the single substrate case. The expressions for the turns ratio n_α in the model [see (14b) or (14c)] depends on the location of the α segment on the cavity surface, on the mode number (via k_x, k_y), and on the segment dimensions. Each different TM_{nmo} resonance will require a new set of circuit components.

When the GCPW cavity is a single layer substrate supporting only T_{mno} modes, the expressions for R, L, C are particularly simple. The arrowed expressions in (16) result from setting $\varepsilon_1 = \varepsilon_2 = \varepsilon' + j\varepsilon''$ and $d_1 + d_2 = d$. The resonance frequency becomes $\omega_0 = c_0[(k_x^2 + k_y^2)/\varepsilon']^{1/2}$ where the reader is reminded that $k_x = n\pi/a$ and $k_y = m\pi/b$. At resonance, the maximum possible mutual admittance between two GCPW segments on a single substrate becomes, $Y_{ij}^{\max} = (n_i n_j)^{\max} Q/(\omega_0 \mu_0 d)$ which shows that resonance coupling is reduced by reducing Q, increasing d, or reducing $(S + W)$ in n_i.

The procedure for evaluating the circuit model is as follows: 1) find ω_0 from (8) for the TM_{nmo} resonance of interest; 2) evaluate the Q of the cavity from (10); 3) evaluate the derivative of Z_m (numerically if necessary); 4) determine R, L, C of the model from (16); 5) divide the circuit into segments; 6) evaluate the turns ratio n_α for the transformer associated with each segment from (16d) and (14b,c) where x_α, y_α is the location of the center of the segment. Lastly the overall circuit model is assembled on a CAD simulator.

III. Comparison to MoM Calculations

In this section we use the circuit model to calculate the effect of a substrate resonance on a single GCPW dipole circuit and then compare the results to a full wave method of moments analysis of the same circuit. The dipole circuit to be analyzed can be described by referring to Fig. 1 except that only one length of GCPW is present and not the two implied by the figure (space limitations preclude a separate figure). The dipole consists of a single 1.05 mm length of GCPW shorted at both ends and fed by an ideal current generator at the center. Its strip and slot widths are $S = 50\mu$m, $W = 25\mu$m. It is centered at $x_j = 2.08$ mm and $y_j = 0.5$ mm and lies in a perfectly conducting plane located at $z = 0$ under which two 125μm thick layers of GaAs ($\varepsilon_r = 12.8$) are located. The upper one has a loss tangent of 0.002 while the lower one has loss tangent of 0.01 for one set of curves and 0.1 for the other set. The lower ground plane is located at $z = -0.25$ mm and is connected to the top plane by perfectly conducting side walls at the edges of the substrate. The cavity thus formed has dimensions $a = 3$ mm and $b = 2$ mm.

Fig. 3 shows the frequency response of the real part of the impedance seen by the current generator. One of the two peaks shown in each trace results from a substrate resonance (the TM_{220} mode) occurring at 50.4 GHz. The other results from the half wave resonance of the dipole itself near 54 GHz.

The circuit model for this structure is the circuit already illustrated in Fig. 2. The GCPW parameters are determined to be

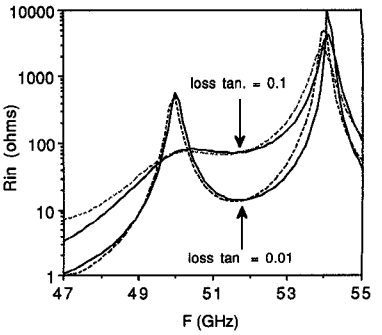

Fig. 3. Full wave method of moments calculation (dashed line) compared to circuit model results (solid line) results when substrate 2 has a loss tangent of 0.01 and 0.1.

$Z = 45.4\Omega, \varepsilon_{\mathrm{eff}} = 6.94$. A phenomenological attenuation factor of 0.16/cm is assumed for reasons to be discussed later. To add the resonance coupling model, the GCPW dipole is divided into three sections. Each section has a length $\Delta\ell = 0.35$ mm and a transformer attached at its center. The centers are located at $x = 1.73, 2.08, 2.43$ mm and $y = 0.5$ mm. Using these values in (14c) gives turns ratios of $n = 0.026, 0.052, 0.052$. Equations (16) give $L = 0.314$ nH, $C = 0.0317$ pf. The Q of the two layer cavity is easily computed via perturbation theory to be $Q \sim 170$ and 20 for the loss tangents 0.01 and 0.1, respectively. Equation (16c) gives resistance of $R = 0.6\Omega$ and $R = 5.0\Omega$, respectively.

To check the accuracy of the modeling, we compare the results to an MoM solution. This solution includes effects such as radiation in the upper half space and loss due to reactive coupling with the substrate below. To account for this in the circuit model we include sufficient attenuation in the model transmission lines to make the peak R_{near} at 54 GHz in the circuit solution equal to the corresponding peak resistance in the full wave solution. No change in this attenuation factor was necessary when the loss tangent was changed. The model and full wave solutions agree remarkably well given the simplicity of the model.

Increasing the number of sections (and transformers) to 4 results in about a 10% change in the peak of R_{in} at 50 GHz. Further increasing the number of sections to 5 results in a negligible change. The number of sections necessary depends on the scale length of change in either the circuits's fields or the resonance mode fields—whichever is smaller. In this case the former is slightly smaller and thus we choose it to be the relevant scale. So in the three section example a result to 10% accuracy was achieved with a section length of roughly 1/6 of a circuit wavelength. Our experience with this experiment therefore suggests that section lengths should be set to 1/6 or less of the smallest relevant wavelength.

IV. Comparison to Experiment

An experimental GCPW circuit was constructed to further test the model's ability to predict resonance coupling. The circuits were fabricated on a high resistivity silicon substrates roughly 10 mm square. The top surface pattern is shown in the inset to Fig. 4 with the shaded areas indicating the lack of conductor. Each circuit consists of a length of CPW transmission line open circuited at each end and probed at an off-center location. The top substrate, with the circuit etched on its upper surface, sits on top of a second high resistivity silicon substrate which in turn sits on top of a metalized ground plane. The total thickness of the substrates sums to 760μm. Silver epoxy paint is used to connect the upper plane to the ground plane at the substrates' perimeter. Thus a $10 \times 10 \times 0.76$ mm cavity is formed. Ideally, no coupling would exist between the two circuits;

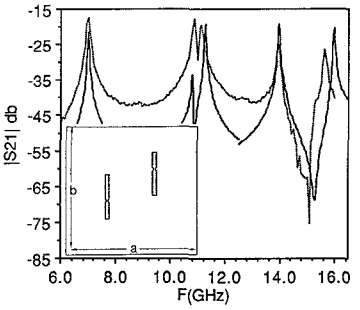

Fig. 4. Measured (···) and modeled (——) transmission results for the experimental two port circuit shown in the inset. Darkened areas in the scale diagram denote 50μm slots in the conducting plane.

however, cavity resonances do cause coupling. We have measured this coupling and compared it to the coupling predicted using the previously described circuit model. Fig. 4 shows the measured results from 6 to 16 GHz. Five resonance peaks are apparent.

More of the specifics of the experiment are as follows. The more accurate lateral dimensions of the chip are $a = 10.4$ mm and $b = 9.74$ mm. The inset figure has been reproduced from the mask we used and is thus to scale (space limitations preclude a more generous figure). Although it is difficult to see, the circuit pattern is shifted upward slightly and thus is not exactly centered on the substrate surface. Each transmission line is 3.3 mm long including the end slots. The center strip width is 200μm except at the probe points. All of the slots, including the ends, are 50μm wide. The gold metallization is $2.5-3\mu$m thick everywhere except in the near vicinity of the CPW where it can be as thin as 1.3μm as a result of the processing technique we used. The bulk dc resistivity of the substrates was measured to be 4.5 ± 1.0 kΩ−cm. This results in a cavity Q of about 200 to 500 over the frequency range of interest. The contribution of conductor loss to the calculated Q is relatively small and has been neglected. The microwave measurements were obtained using a Cascade prober and an HP-8510 system.

In applying the circuit model to this structure, we assumed a dielectric constant of 11.8 for the silicon and found that theoretically the lowest order resonance should occur at 6.14 GHz. Instead it is measured at 7.0 GHz. We account for this by assuming a physically plausible 22 micron air gap between the lowest substrate and the ground plane. This shifts the lowest order model resonance up so that it lines up with the measurement. All the other resonances then line up fairly well.

It turns out that the model predicts that the coupling results primarily from the slots which form the open circuit at the end of each transmission line and not from the coplanar waveguide in the middle. As a result, each model transmission line has a transformer attached at each end—four total for modeling a single resonance. In the case of the 7.0 GHz resonance the circuit elements were $R = 0.21\Omega$, $L = 0.97$ nH, $C = 0.53$ pF, and $n = 0.020, 0.005, 0.011, 0.024$. The turns ratios are listed for each slot starting from the bottom and progressing in order to the top of the inset to Fig. 4. Note that calculating the transformer ratios from (14b) gives negative values for the least two values listed. The sign of these values was switched to reflect the different orientation of the voltage polarity defined at the upper ends of each line. Also the length of the modeled slot $\Delta\ell$ was chosen to be 250 microns instead of 300 to reflect the fact that the fringe slot fields turn at the corners of the open end. The resulting circuit model is similar to Fig. 2 except that two transmission lines are present with the end of each line terminated with a transformer primary and the four secondaries form a loop with a RLC circuit.

The model results in Fig. 4 were first computed from 6 to 12 GHz and then from 12 to 16.5 GHz. There are three resonances in the first range and thus the model has three tank circuits/transformer sets in it. The agreement between theory and experiment is good at two out of the three resonances. There are also three resonances in the second range, but the model predicts that one of them, the [3, 1] resonance at 15.2 GHz, would not couple significantly and thus it was left out of the model. The measurement confirms the negligible effect of the [3, 1] resonance although a small peak is just visible. The remaining two peaks are off by about 6 dB from the model. We attribute this to a reduced Q at each of the resonances due to the fact that the slot line mode of the CPW line becomes resonant near 17 GHz and thus increased radiation occurs. We think that this radiation occurs as a result of the slot line being incompletely shorted by wire bonds. Note that the dip in measured response occurring at 15 GHz is reproduced by the model. This dip results from the interaction between the [2, 2] and [3, 1] modes.

The measured results agree reasonably well with the model when one takes into account the uncertainties in loss and the possibly uneven air gap that evidently exists.

V. Conclusion

In the previous sections a simple circuit model for resonance coupling in GCPW circuits has been described and verified by comparison with full wave simulation and with experiment.

The principal advantage of this model is its simplicity. The components of the model can be calculated with a hand calculator in many cases. It makes it possible to include the effect of a substrate resonance in with a circuit CAD model without resorting to an electromagnetic simulator. This will be useful as a diagnostic tool, showing "hot" coupling spots and providing bounds on the seriousness of a resonance coupling effect.

The modeling scheme can become unwieldy if it is not used carefully. A large number of transformers may be necessary if more than a couple resonances are modeled at once or if a large circuit with many sections must be modeled. In calculating the model for large circuits it usually becomes apparent that many sections of a circuit do not couple significantly and thus their transformers need no be included. For example, slots or components with unbalanced field structures couple to a resonance much more effectively than CPW components. Thus anytime slot-like coupling is likely to occur, a first cut model would include it and neglect CPW coupling.

If very accurate coupling estimates are necessary, the Q of the GCPW cavity must be accurately known. In practical cases this may be difficult since substrate loss may not be accurately known and other losses may be difficult to quantify. One such loss is the radiation loss resulting from incompletely short circuited side-walls. Also, substrate resonance fields may excite the undesirable "even" CPW mode in the surface circuitry. If such modes are incompletely air bridged, they can radiate and reduce Q.

From a circuit point of view one wants to reduce the substrate resonance Q since this reduces the undesirable mutual admittance between circuit components. Since the losses mentioned above may not be repeatable from circuit to circuit, it may be better to include lossy material at the edges of a substrate, or to include a lossy sub-substrate as described in Section III (doped silicon is a lower cost alternative with much higher thermal conductivity). As is the case for coupling to parallel plate waves in a laterally open substrates [2]–[5], [8], a thicker substrate and smaller GCPW cross-section will reduce coupling to resonant mode fields.

VI. Appendix

The derivation of Green's functions of this type is fairly well known and the details are not presented here. The following Green's functions relates an x or y directed magnetic current located on the $z = 0^-$ plane of Fig. 1 to the H_x field on the same plane.

$$G_{xx}(x,x',y,y') = \sum_{n=1}^{\infty}\sum_{m=1}^{\infty} \frac{4}{abk_\rho^2}\left(\frac{k_x^2}{Z_E} + \frac{k_y^2}{Z_M}\right) \cdot \cos(k_y y)\ \cos(k_y y')\ \sin(k_x x)\ \sin(k_x x')$$

$$G_{xy}(x,x',y,y') = \sum_{n=1}^{\infty}\sum_{m=1}^{\infty} \frac{-4k_x k_y}{abk_\rho^2}\left(\frac{1}{Z_E} - \frac{1}{Z_M}\right) \cdot \sin(k_y y)\ \cos(k_y y')\ \cos(k_x x)\ \sin(k_x x') \tag{A1}$$

where

$$k_x = \frac{n\pi}{a}, \qquad k_y = \frac{m\pi}{b},$$
$$k_\rho^2 = k_x^2 + k_y^2, \qquad k_i = \sqrt{\varepsilon_{ri}k_0^2 - k_\rho^2}$$
$$Z_V = jZ_{TV1}\frac{Z_{TV2}\ \tan(k_2 d_2) + Z_{TV1}\ \tan(k_1 d_1)}{Z_{TV1} - Z_{TV2}\ \tan(k_2 d_2)\ \tan(k_1 d_1)} \tag{A2}$$

where

$$Z_{TMi} = \frac{k_i \eta_0}{\varepsilon_{ri}k_0}, \qquad Z_{TEi} = \frac{k_0\eta_0}{k_i},$$
$$V = E \quad \text{or} \quad M, \qquad i = 1 \quad \text{or} \quad 2.$$

Acknowledgment

The author is grateful to M. M. Goldberg for very patiently fabricating and measuring the experimental circuits described in this paper.

References

[1] R. Majidi *et al.*, "5-100 GHz InP CPW MMIC 7-section distributed amplifier," in *IEEE Monolithic Circuits Symp. Dig.*, May 1990, pp. 31–34.
[2] H. Shigesawa, M. Tsuji, and A. A. Oliner, "Conductor-backed slot-line and coplanar waveguide: Dangers and full wave analyses," in *IEEE MTT-S Microwave Symp. Dig.*, 1988, pp. 199–202.
[3] R. W. Jackson, "Mode conversion at discontinuities in modified grounded coplanar waveguides," in *IEEE MTT-S Int. Microwave Symp. Dig.*, 1988, pp. 203–206.
[4] ——, "Mode conversion at discontinuities in finite-width conductor-backed coplanar waveguide," *IEEE Trans. Microwave Theory Tech.*, vol. 37, pp. 1582–1588, Oct. 1989.
[5] M. Riaziat *et al.*, "Single mode operation of coplanar waveguides," *Electron. Lett.*, vol. 23, Nov. 19, 1987.
[6] R. W. Jackson, "Considerations in the use of coplanar waveguide for millimeter-wave integrated circuits," *IEEE Trans. Microwave Theory Tech.*, vol. MTT-34, pp. 1450–1455, Dec. 1986.
[7] J. J. Burke and R. W. Jackson, "A simple circuit model for resonant mode coupling in packaged MMICs," in *IEEE MTT Symp. Dig.*, Boston, MA, June 1990.
[8] E. Godshalk, "Wafer probing issues at millimeter wave frequencies," in *Proc. European Microwave Conf.*, 1992, pp. 925–930.

CPW Oscillator Configuration for an Electro-Optic Modulator

Vesna Radišić, Vladan Jevremović, Zoya Basta Popović

***Abstract*— A CPW 2 GHz 3-port MESFET oscillator was designed with an electro-optic modulator application in mind. The oscillator has a self-biased gate. The source or drain ports can be used for external injection-locking. The frequency of oscillation, as well as the output power at the fundamental and first two harmonics were analyzed using a nonlinear device model and a harmonic balance technique. Comparison with measured results on a hybrid CPW oscillator fabricated on a Duroid substrate are presented.**

I. Introduction

Recently, there has been great interest in gigabit modulation of guided optical signals for high data rate communications. A Mach–Zehnder modulator with electrodes in a push/pull configuration, fabricated with both SiO_2 and SiN buffer layers and indium tin oxide (ITO) was reported in [1]. The difficulty in the operation of wideband modulators is that the modulation is performed with an applied voltage. For a practical modulation index this voltage needs to be at least 5 V. The necessary modulating power decreases dramatically with the electrode structure. Izutsu *et al.* [2] presented a three-electrode coplanar waveguide modulator with a short circuited resonant line for the modulating electrode. Another analysis of CPW for $LiNbO_3$ optical modulators was presented in [3], but no active modulators for this purpose have been reported in the literature. The purpose of designing the CPW oscillator presented in this work is an efficient, compact, low power, active modulator with an open circuited resonant line for the modulating electrode. A 2-port superconductive CPW oscillator has been reported in the literature [4], but the approach taken here was to design a 3-port oscillator, and use the additional port for external injection-locking.

CPW is an attractive guiding medium for this application for a variety of reasons. Since the microwave voltage is applied between the central electrode and coplanar ground planes, many layers can potentially be stacked for dense electro-optic interconnects. The ground planes act as a good heat sink and monolithic implementation is compatible with active device layout, so that no via-holes are required. Further, although the widths of the gap and inner conductor are not fixed for a given impedance, their ratio is fixed. This allows for flexible design and high frequency operation.

II. Design, Analysis and Measurement of the CPW Oscillator

The oscillator configuration is shown in Fig. 1. The analysis of the oscillator was done on Hewlett Packard's Microwave Design System (MDS) using transmission line circuit modeling. The device is a Fujitsu GaAs MESFET (FSC11FA/LG), which is a low noise device for C-band satellite communication receivers. The gate of the device is self-biased in order to minimize the number of bias points. The source and the drain are connected to 50Ω transmission lines. If needed, an additional bias line can be added at an appropriate place along the gate resonator. Since the gate is self-biased, and therefore the transistor is deep in saturation, a nonlinear analysis was performed.

Manuscript received September 20, 1992; revised February 1, 1992.
The authors are with the Department of Electrical and Computer Engineering, University of Colorado, Boulder, CO 80309-0425.
IEEE Log Number 9211843.